Radiation Report
Single-Event Effects Test Report of the TPS7H2201-SP

TEXAS INSTRUMENTS

ABSTRACT

The purpose of this study was to characterize the single-event effect (SEE) performance due to heavy-ion irradiation of the TPS7H2201-SP. Heavy-ions were used to irradiate six devices in 14 runs with a flux of approximately 10^5 ions / cm^2 × s and fluence of approximately 10^7 ions / cm^2. The results demonstrate that the TPS7H2201-SP is SEL, SEB, SEGR, SET, and SEFI free up to LET_{EFF} = 75 MeV·cm^2/mg (at 125°C for SEL and 25°C for SET, SEB, SEGR, and SEFI), and across the full electrical specifications. This report uses the QMLV TPS7H2201-SP device in a ceramic package. It is also applicable for the QMLP TPS7H2201-SP device in a plastic package which uses the same die as the QMLV device.

Table of Contents

Trademarks

Kevlar® is a registered trademark of E.I. du Pont de Nemours and Company.
LabVIEW® is a registered trademark of National Instruments.
All trademarks are the property of their respective owners.

1 Device Overview

The TPS7H2201-SP is a space grade, radiation-hardened, 1.5 to 7 V, 6 A ,e-fuse. The device contains a P-channel MOSFET as the switch element. The device supports a maximum of six amps of continuous current and provides a programmable current limit pin and fast current trip for overcurrent load protection. Additional features of the device include the following:

- Programmable soft start (used to limit the inrush current)
- Reverse current protection
- Programmable fault timers for current limit and re-try modes
- Thermal shutdown
- Programmable EN and OVP voltage
- A pin (CS) that outputs a current proportional to the current across the pass element for health monitoring

The device is offered in a thermally enhanced 16-pin ceramic, dual in-line flat-pack package. Table 1-1 lists the general device information and test conditions. See the TPS7H2201-SP product page for more detailed technical specifications, user guides, and applications notes.

Table 1-1. Overview Information

| Description	Device Information
TI Part Number	TPS7H2201-SP
SMD Number	5962R1722001VXC
Device Function	eFuse
Technology	250 nm Linear BiCMOS 7
Exposure Facility	Radiation Effects Facility, Cyclotron Institute, Texas A&M University
Heavy Ion Fluence per Run	$\geq 1 \times 10^7$ ions / cm^2
Irradiation Temperature	25°C and 125°C (for SEL testing)

2 Single-Event Effects

The primary destructive single-event effect (DSEE) events of interest in the TPS7H2201-SP are single-event latch-up (SEL), single-event burn-out (SEB), and single-event gate rupture (SEGR). In mixed technologies such as the Linear BiCMOS 7 process used for the TPS7H2201-SP, the CMOS circuitry introduces a potential for SEL, SEB, and SEGR susceptibility.

SEL can occur if excess current injection caused by the passage of an energetic ion is high enough to trigger the formation of a parasitic cross-coupled PNP and NPN bipolar structure (formed between the p-sub and n-well and n+ and p+ contacts) [1, 2]. The parasitic bipolar structure initiated by a single-event creates a high-conductance path (inducing a steady-state current that is typically orders-of-magnitude higher than the normal operating current) between power and ground that persists (is *latched*) until power is removed or until the device is destroyed by the high-current state. For the design of the TPS7H2201-SP, SEL-susceptibility was reduced by maximizing anode-cathode spacing (tap spacing) while increasing the number of well and substrate ties in the CMOS portions of the layout to minimize well and substrate resistance effects. Additionally, junction isolation techniques were used with buried wells and guard ring structures isolating the CMOS p-wells and n-wells (3, 4). The design techniques applied for SEL-mitigation were sufficient as the TPS7H2201-SP exhibited absolutely no SEL with heavy-ions of up to LET_{EFF} = 75 MeV-cm^2 / mg at fluences in excess of 10^7 ions / cm^2 and a die temperature of 125°C.

SEB is similar to the SEL and occurs when the parasitic BJT of the DMOSFET is turned on by the heavy-ion strike. DMOS are susceptible to SEB and SEGR while on the off state, however, for the sake of sanity, the device was also evaluated on all possible cases (enable and disable). When a heavy ion with sufficient energy hits the p body, it creates an excess charge inducing a voltage drop. This voltage drop forward biases the emitter-base junction of the parasitic NPN (formed by the N+ source, the P base region, and the N-drift region). If this happens when the DMOSFET is under a high drain bias, a secondary breakdown of the parasitic npn BJT can occur, creating permanent damage of the DMOS (6). When the heavy-ion hits the neck region of the DMOS (under the gate), it creates electron hole-pairs on the oxide and silicon. Drift separates the excess electrons and holes due to the positive bias field on the drain to source of the DMOS. Holes are driven upward to the dioxide while the electrons are transported toward the drain. The collected holes on the dioxide create an equal image of electrons on the opposite side of the gate dioxide. Since the charge injection and collection after an event is faster than the transport and recombination of the e-h pairs, a voltage transient can be developed across the gate oxide. If this build-up voltage is higher than the oxide breakdown, permanent damage can be induced on the oxide, creating a destructive gate rupture (7). The TPS7H2201-SP was tested for SEB and SEGR at LET_{EFF} = 75 MeV-cm^2 / mg, fluences of ≥ 10^7 ions/cm^2, die temperature of 20–25°C, and V_{IN} = 7 V. No increment on the V_{IN} current was observed, also any functionality malfunction was observed, demonstrating that the TPS7H2201-SP is SEB and SEGR-free.

3 Test Device and Evaluation Board Information

The TPS7H2201-SP is packaged in a 16-pin thermally-enhanced dual ceramic flat pack package (HKH) as shown in Figure 3-1. The TPS7H2201EVM-CVAL evaluation board was used to evaluate the performance and characteristics of the TPS7H2201-SP under heavy-ions. Figure 3-2 shows the top and bottom views of the evaluation board used for the radiation testing. Figure 3-3 shows the board schematics. See the TPS7H2201-SP Single Evaluation Module for more information about the evaluation board.
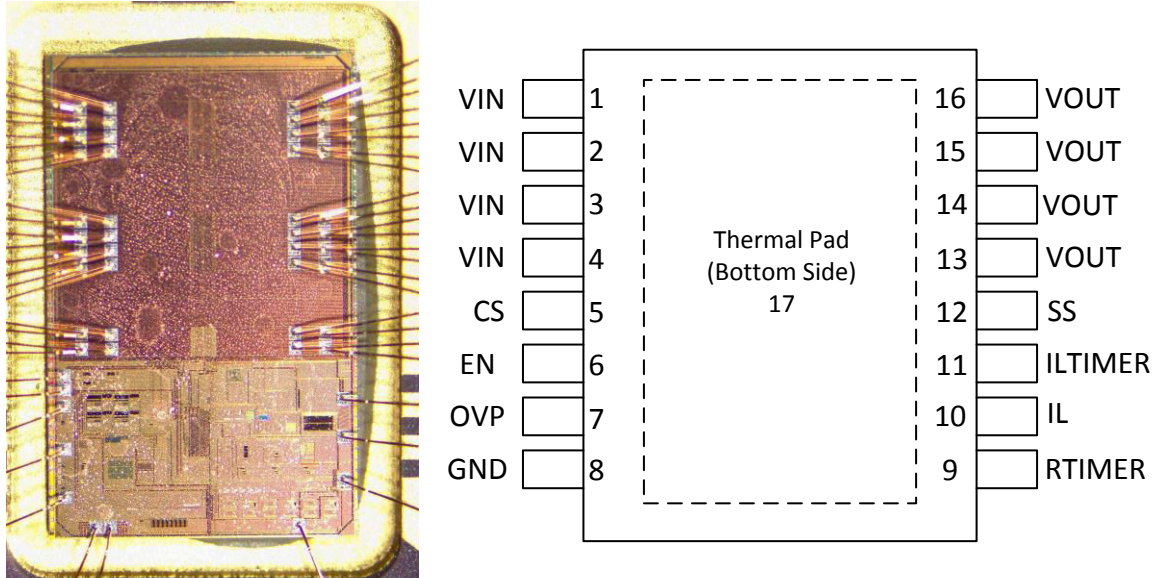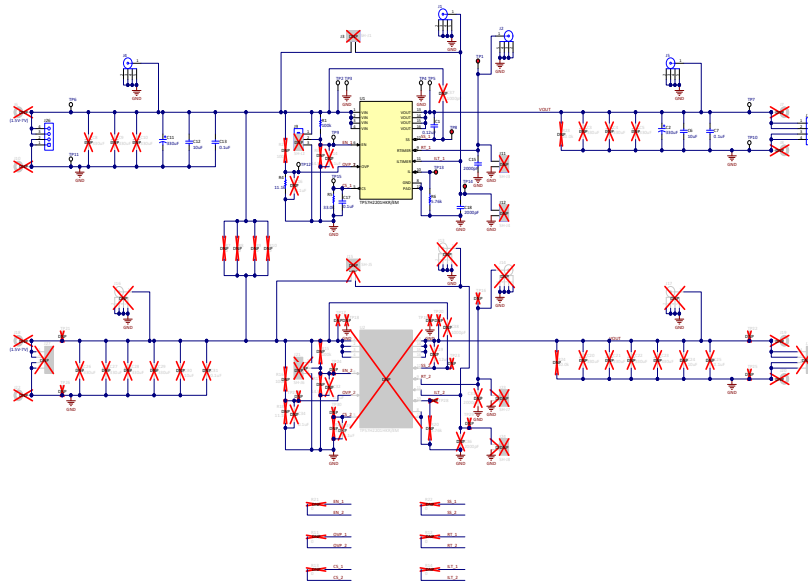

The package lid was removed to reveal the die face for all heavy ions testing

**Figure 3-1. Photograph of Delidded TPS7H2201-SP (Left) and Pin Out Diagram (Right)**
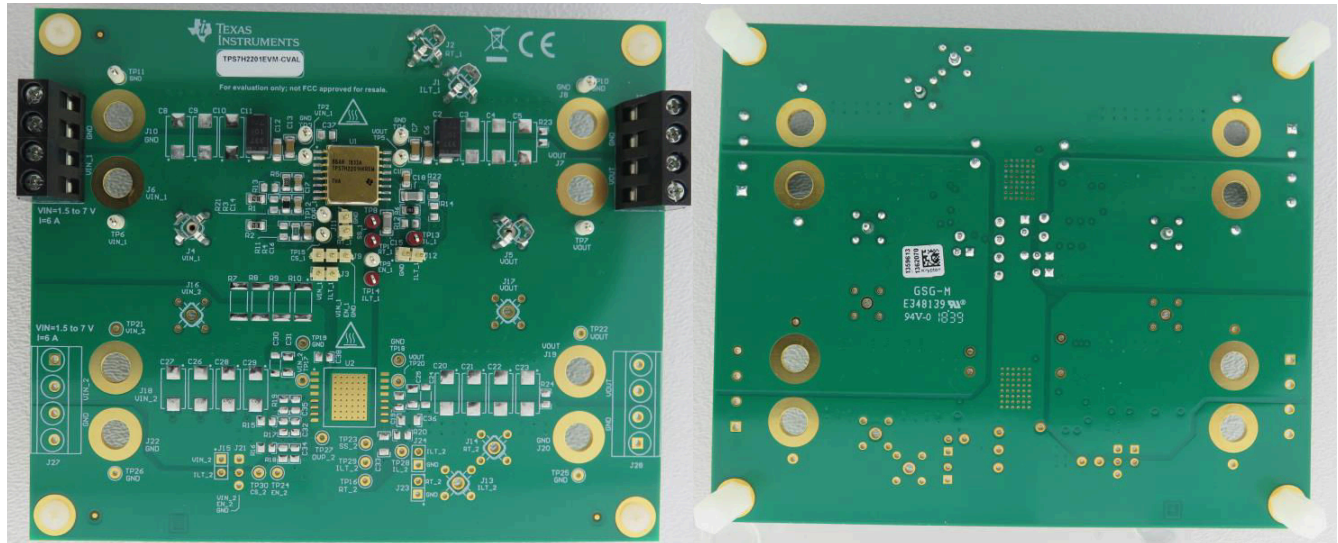
Figure 3-2. TPS7H2201-SP Board Top View (Left) and Bottom-View (Right)

R2, R3, C14, and C16 are populated components on the TPS7H2201EVM-CVAL, however, the components were removed and all boards used for the characterization discussed in this report had the switch closed during most of the SEE characterization.

Figure 3-3. Schematics of the TPS7H2201EVM-CVAL Used for the Heavy-ion Testing

4 Depth, Range, and LET$_{EFF}$ Calculation
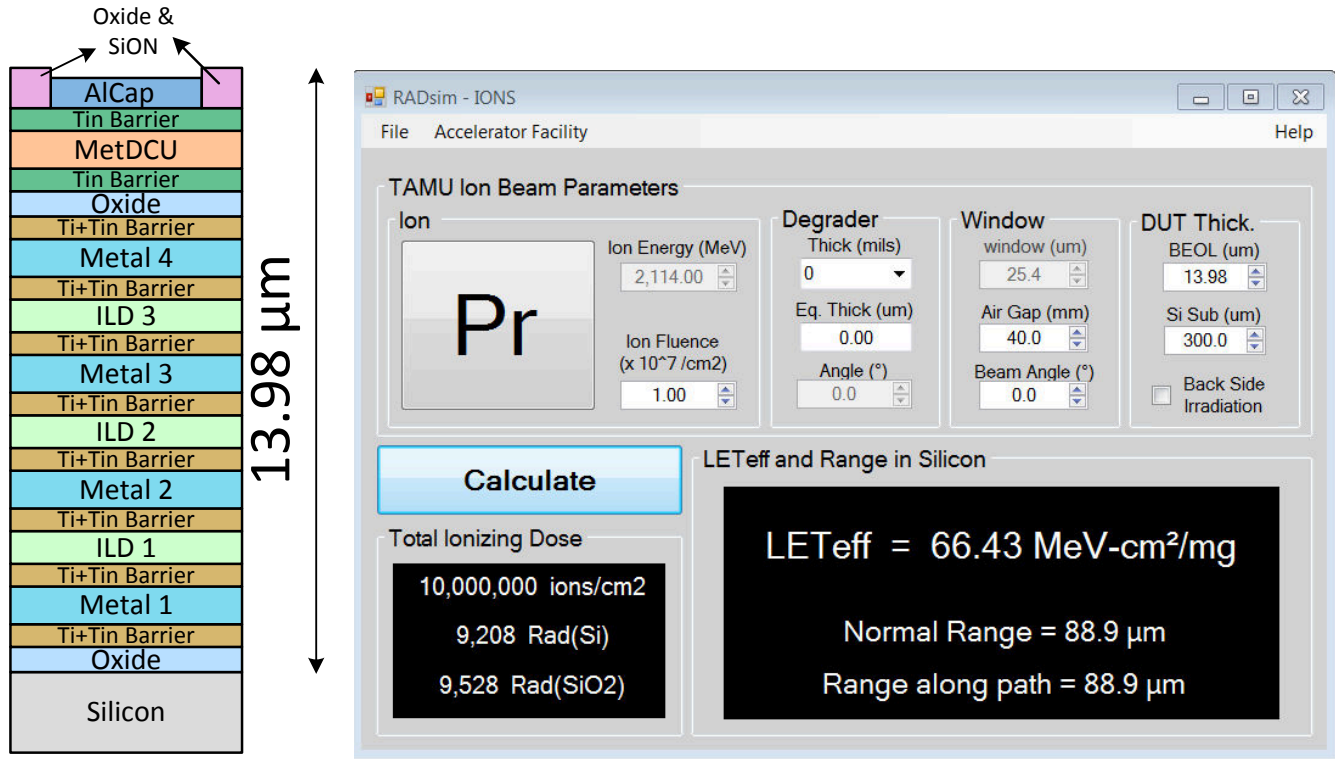
Figure 4-1. Generalized Cross-Section (Left) of the LBC7 Technology BEOL Stack on the TPS7H2201-SP. GUI of RADsim Application (Right)

The TPS7H2201-SP is fabricated in the TI Linear BiCMOS 7, 250 nm process with a back-end-of-line (BEOL) stack consisting of four levels of aluminum. The total stack height from the surface of the passivation to the silicon surface is 13.98 µm based on nominal layer thickness as shown in Figure 4-1. Accounting for energy loss through the 1 mil thick Aramica (Kevlar®) beam port window, the 40-mm air gap, and the BEOL stack over the TPS7H2201-SP, the effective LET (LET$_{EFF}$) at the surface of the silicon substrate and the depth and ion range was determined with the custom RADsim-IONS application (developed at Texas Instruments and based on the latest SRIM2013 [9] models). Table 4-1 lists the results.

Table 4-1. Praseodymium Ion LET$_{EFF}$, Depth, and Range in the TPS7H2201-SP

Ion Type	Angle of Incidence (°)	Depth in Silicon (µm)	Range in Silicon (µm)	LET$_{EFF}$ (MeV·cm^2 / mg)
Pr	0	88.9	88.9	66.43
Pr	27.3	77.7	87.2	75

5 Irradiation Facility and Setup

The heavy-ion species used for the SEE studies on this product were provided and delivered by the Texas A&M University (TAMU) Cyclotron Radiation Effects Facility (8) using a superconducting cyclotron and advanced electron cyclotron resonance (ECR) ion source. At the fluxes used, ion beams had good flux stability and high irradiation uniformity over a 1" diameter circular cross sectional area for the in-air station. Uniformity is achieved by means of magnetic defocusing. The flux of the beam is regulated over a broad range spanning several orders of magnitude. For the bulk of these studies, ion flux of approximately 10^5 ions / cm^2 × s were used to provide heavy-ion fluences ≥ 10^7 ions / cm^2.

For the experiments conducted on this report, ^{141}Pr ions at angles of 0° and 27.3° of incidence were used for an LET$_{EFF}$ of 66.43 and 75 MeV × cm^2 / mg, respectively. The total kinetic energy of ^{141}Pr on the vacuum is 2.114 GeV. Ion uniformity for these experiments was between 81% and 98%.

Figure 5-1 shows the TPS7H2201-SP test board used for the experiments at the TAMU facility. Although not visible in this photo, the beam port has a 1-mil Aramica window to allow in-air testing while maintaining the vacuum within the accelerator with only minor ion energy loss. Test points were soldered on the back for easy access of the signals while having enough room to change the angle of incidence and maintaining the 40 mm distance to the die. The air space between the device and the ion beam port window was maintained at 40 mm for all runs.
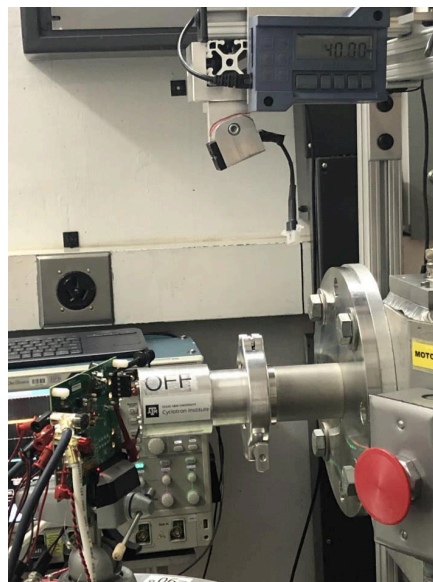
Figure 5-1. Photograph of the TPS7H2201-SP Mounted on the TPS7H2201EVM-CVAL in Front of the Heavy-ion Beam Exit Port at the TAMU Accelerator Facility

6 Test Setup and Procedures

SEE testing was performed on a TPS7H2201-SP device mounted on a TPS7H2201EVM-CVAL. The device power was provided to the VIN-GND input on the J26 terminal block inputs using the N6702 precision power supply (PS) in a 4-wire configuration. For the SEL, SEB, and SEGR testing, the device was powered up at seven volts and loaded with approximately 1.1-Ω discrete resistors (six amps). The V_{OUT} under this condition was 6.76 volts. For the SEB and SEGR characterization, the device was tested under enabled and disabled modes. An NI PXI-4110 PS was used to control the EN voltage to enable and disable the DUT. The discrete resistive load was connected even when the DUT was disabled to help differentiate events during testing. Not a single current increment event was observed during any of the SEL, SEB, and SEGR testing.

For the SET characterization, the device was powered up at minimum and maximum recommended voltages of 1.5 V and 7 V, and loaded to the maximum six amps using discrete resistors.

All equipment was controlled and monitored using a custom-developed LabVIEW® program (PXI-RadTest) running on a NI-PXIe-8135 controller. The current of the power supply, the temperature and the beam start and stop (5-V tamu signal) signal were monitored at all times and logged for further analysis.

Figure 6-1 shows a block diagram of the setup used for SEE testing of the TPS7H2201-SP. Table 6-1 shows the connections, limits, and compliance used on the test equipment. For the SEB/SEGR characterization, the die temperature was maintained between 20°C to 25°C by using a vortex tube to cool down the device when needed (when the part was enabled and loaded to 6-A). A die temperature of 125°C was used for SEL testing and was achieved by attaching three parallel power resistors (model: RP60800R0100JNBK) to the thermal pad on the back of the board using solder paste. The die temperature was monitored during the testing using a K-Type thermocouple attached to the heat slug of the package, and correlated using a thermal camera before the SEE characterization. As observed on Figure 6-1, two scope cards were used to trigger from V_{OUT} and SS in case of a transient. The scope card triggering from V_{OUT} was also monitoring VIN, CS, R_{TIMER}, and IL_{Timer}. The trigger used was a window set at ±3 % around the nominal output voltage (when the device was enabled) and ±200 mV (when the device was disabled). The scope card was set with a sample rate of 5 MS / s , record length of 60 kS per record and reference of 20%. A reference of 20% means that in case a trigger occurs, the 20% (12 kS) of the data before the time the trigger occurred was saved. For the scope card, triggering from SS the V_{OUT} was also monitored. The trigger type used for SS was a edge positive trigger set at 500 mV. The scope card was set 2 MS / s, record length of 60 kS per record and 20% reference. Both scope cards were continuously monitoring the trigger signals and data was saved only if this signal exceeded the trigger set on the scope card.

All boards used for SEE testing were fully checked for functionality and dry runs were performed to make sure that the test system was stable under all bias and load conditions prior to being taken to the TAMU facility. During the heavy-ion testing, the LabView control program (PXI-RadTest) powered up the TPS7H2201-SP device and set the external sourcing and monitoring functions of the external equipment. After functionality and stability were confirmed, the beam shutter was opened to expose the device to the heavy-ion beam. The shutter remained open until the target fluence was achieved (determined by external detectors and counters).

Table 6-1. Equipment Set and Parameters Used for the SEE testing of the TPS7H2201-SP

Pin Name	Equipment Used	Capability	Compliance	Range of Values Used
V_{IN}	Agilent N6702A (Channels 2 and 3 in parallel)	10 A	10-A	1.5 and 7 V
EN	ni-PXIe-4110 (Channel 1)	1 A	0.1-A	0 and 1 V
Digital I/O	NI PXIe 6556	200 MHz	—	50 MHz
Vout	NI PXIe 5105	60 MHz	—	5 MHz
SS	NI PXIe 5105	60 MHz	—	2 MHz
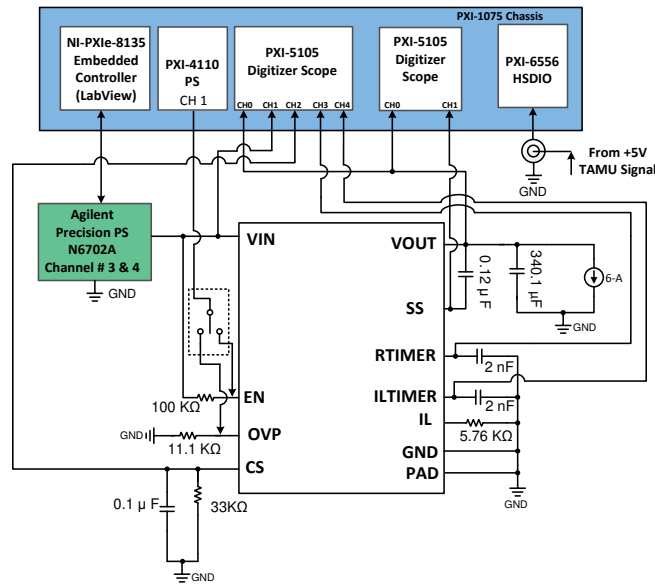
Figure 6-1. Block Diagram of SEE Test Setup Used for the TPS7H2201-SP Characterization

The single pole, double throw (SPDT) switch shown on the EN pin was not a physical connector present during the testing. However, the SPDT is used here to represent the possible ways the EN and OVP pins were biased to disable the device during the characterization.

7 Single-Event-Latchup (SEL), Single-Event-Burnout (SEB), and Single-Event-Gate-Rupture (SEGR)
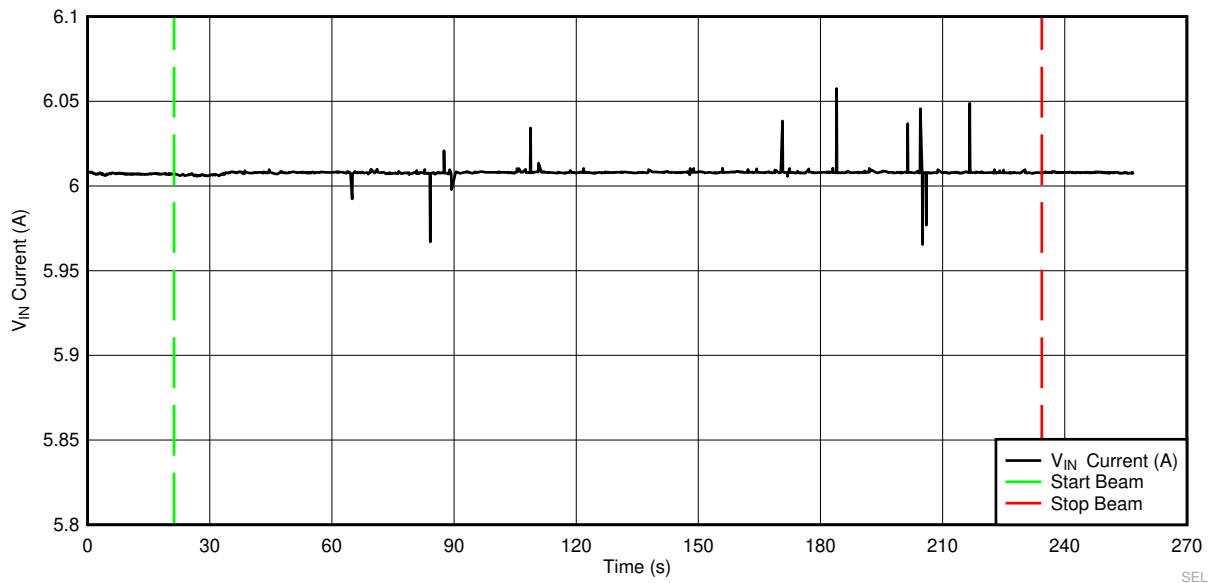
7.1 Single-Event-Latchup (SEL)

All SEL characterizations were performed with die temperature of 125°C. The device was heated by connecting three parallel power resistors (model: RP60800R0100JNBK) attached with thermal paste to the back of the board. The temperature was monitored by attaching a K-type thermocouple to the thermal pad of the device on the top layer. Thermocouple and die correlation was verified by using a thermal IR camera, prior to reach to the heavy-ions facility (TAMU).

The device was exposed to a Praseodymium (Pr) heavy-ion beam incident on the die surface at 0° and 27.3° for an LET_{EFF} of 66.43 and 75 MeV-cm^2 / mg, respectively. Flux of approximately 10^5 ions / cm^2 × s and fluence ≥ 10^7 ions / cm^2 was used in each run. Run duration to achieve this fluence was approximately two minutes (for 10^7 ions / cm^2). During the SEL testing, the device was set up as described in Figure 3-3. Table 7-1 summarizes the SEL results. No SEL events were observed under any of the test runs, indicating that the TPS7H2201-SP is SEL-immune at T = 125°C and LET = 75 MeV·cm^2 / mg. SEL cross-section was calculated based on 0 events observed using a 95% (2σ) confidence interval (see Section 11 for discussion of cross-section calculation method). Figure 7-1 shows a typical current plot.

$$\sigma_{SEL} \leq 1.84 \times 10^{-7} cm^2 / device \text{ for } LET_{EFF} = 75 MeV \times cm^2 / mg \text{ and } T_J = 125°C, 95\% \text{ conf}. \qquad (1)$$

Table 7-1. Summary of TPS7H2201-SP SEL Results With T = 125°C and LET_{EFF} = 74.83 MeV-cm^2/ mg

Run Number	Unit Number	Temperature (°C)	Ion Type	Angle of Incidence (°)	LET_{EFF} (MeV × cm^2 / mg)	Flux (ions / cm^2 × s)	Fluence (ions / cm^2)	VIN (V)	Load (A)	SEL Events
1	1	125	Pr	27.3	75	1.07×10^5	2×10^7	7	6	0
2	1	125	Pr	0	66.43	1.14×10^5	9.95×10^6	7	6	0

Figure 7-1. Current Versus Time for SEL Run 1 at T = 125°C and 75 MeV × cm^2/ mg

7.2 Single-Event-Burnout (SEB) and Single-Event-Gate-Rupture (SEGR)

SEB and SEGR were performed at room temperature, with [141]Pr with an angle of incidence of 0° and 27.3° die for an LET_{EFF} of 66.43 and 75 MeV × cm^2 / mg, respectively. The V_{IN} was held at the maximum recommended voltage of 7 V. Flux of approximately 10^5 ions / cm^2 × s and fluence ≥ 2 × 10^7 ions / cm^2 was used in each run. The device was evaluated when the DUT was enabled and disabled, and loaded to 6 A at all times. Even when the device was disabled, the device was loaded (6 A) to help identify if the device was changing modes or closing the switch (disabled to enabled), due to heavy-ions. When the DUT was disabled, the die temperature was at room temp (approximately 23°C), however, when the part was enabled and loaded with six amps, the power dissipated across the pass element increments the die temperature. To test the device around (20°C to 25°C), an external cool element (vortex tube) was used. The stream of cold air was pointed at the die to chill the device during the testing. No change on current was observed, indicating that the TPS7H2201-SP is SEB and SEGR immune at T = 25°C and LET = 75 MeV × cm^2 / mg. During the SEB and SEGR testing with the switch disabled the current never increment, indicating that the device never changed status during the exposure. Table 7-2 lists the conditions used for this test. Figure 7-2 shows a typical V_{IN} current versus time plot. The SEB and SEGR cross-section was calculated based on 0 events observed using a 95% (2σ) confidence interval and combining (or summing) fluences (see Section 11 for discussion of confidence limits).

$$\sigma_{SEB/SEGR} \leq 4.61 \times 10^{-8} cm^2/device \text{ for } LET_{EFF} = 75 MeV \times cm^2/mg \text{ and } T_J = 25°C, \text{ 95\% conf.} \qquad (2)$$

Table 7-2. Summary of TPS7H2201-SP SEB and SEGR Results with T = Approximately 25°C

Run Number	Unit Number	Temperature (°C)	Ion Type	Angle of Incidence (°)	LET$_{EFF}$ (MeV × cm^2 / mg)	FLUX (ions / cm^2 × s)	FLUENCE (ions / cm^2)	VIN (V)	Load (A)	Enabled?	SEB or SEGR Events
3	1	25	Pr	27.3	75	1.08 × 10^5	2 × 10^7	7	6	Yes	0
4	2	20	Pr	27.3	75	1.28 × 10^5	3 × 10^7	7	6	Yes	0
5	2	20	Pr	27.3	75	1.16 × 10^5	3 × 10^7	7	6	No	0
6	3	25	Pr	0	66.43	1.07 × 10^5	2.01 × 10^7	7	6	Yes	0
7	3	25	Pr	0	66.43	1.03 × 10^5	2 × 10^7	7	6	No	0
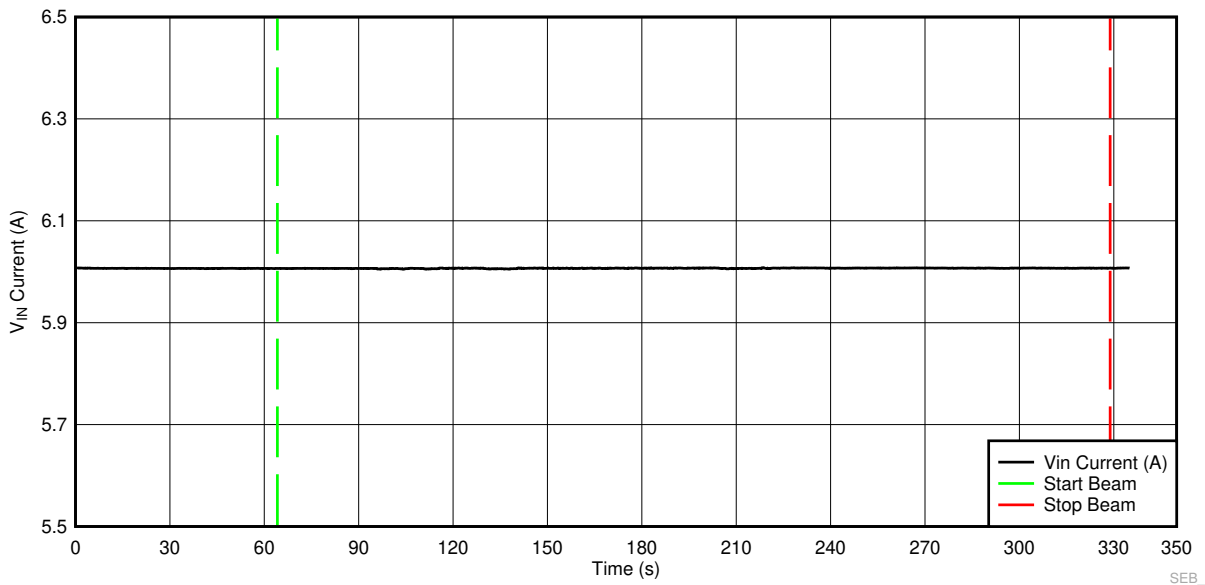
Figure 7-2. Current Versus Time for SEB and SEGR Run 4 at T = 20°C and 75 MeV × cm^2 / mg

8 Single Event Transient (SET)

SET testing was performed at room temperature, with[141]Pr with an angle of incidence of 27.3° die for a LET_{EFF} 75 MeV × cm^2/ mg. The V_{IN} was set to maximum (7-V) and minimum (1.5-V) recommended voltages at maximum load of 6-A and no load. Under these conditions, the die temperature is around 33 °C when loaded to 6-A and 23°C when not loaded. Flux of approximately 10^5 ions /cm^2× s and fluence ≥ 1× 10^7 ions / cm^2 were used in each run. The device was also evaluated when the DUT was disabled by using the EN (0-V) and the OVP (1-V) pins by forcing an external voltage into the pins. Not a single upset on Vout or SS was observed during the SET testing at room temperature. A window trigger with ±3% around the output nominal voltage (when the device was enabled) and a ±200 mV (when the device was disabled) was used for the detection of upsets during the characterization.

During the SEL testing, when the device was exposed to a die temperature of 125°C, upsets that create a momentary Soft Start (SS) cycle were observed. Table 8-1 lists the test conditions and results for the SET testing of the TPS7H2201-SP. Worst case observed transient (SET) for V_{OUT} and SS is shown in Figure 8-1.

The SET cross-section was calculated observed 95% (2σ) confidence interval and combining (or summing) fluences (see Section 11 for discussion of confidence limits). The cross section is classified by die temperature and LET_{EFF}.

$$\sigma_{SET} \le 2.29 \times 10^{-8} cm^2/device \text{ for } LET_{EFF} = 75 MeV \times cm^2/mg \text{ and } T_J = 33°C, \text{ 95% conf.} \tag{3}$$

$$\sigma_{SET} \le 2.18 \times 10^{-5} cm^2/device \text{ for } LET_{EFF} = 75 MeV \times cm^2/mg \text{ and } T_J = 125°C, \text{ 95% conf.} \tag{4}$$

$$\sigma_{SET} \le 1.17 \times 10^{-6} cm^2/device \text{ for } LET_{EFF} = 66.43 MeV \times cm^2/mg \text{ and } T_J = 125°C, \text{ 95% conf.} \tag{5}$$

Table 8-1. Summary of TPS7H2201-SP SET Results With T = Approximately 25°C and 125°C

| Run Number	Unit Number	Temperature (°C)	Ion Type	Angle of Incidence (°)	LET_{EFF} (MeV × cm^2 / mg)	Flux (ions / cm^2 × s)	Fluence (ions / cm^2)	VIN (V)	Load	Enabled?	SET Events
8	3	33	Pr	27.3	75	9.94 × 10^4	2 × 10^7	7	6	Yes	0
9	3	33	Pr	27.3	75	9.97 × 10^4	2 × 10^7	7	0	Yes	0
10	4	33	Pr	27.3	75	1.01 × 10^5	2 × 10^7	1.5	6	Yes	0
11	4	33	Pr	27.3	75	1.09 × 10^5	2 × 10^7	1.5	0	Yes	0
12	3	33	Pr	27.3	75	1.04 × 10^5	2 × 10^7	7	6	No	0
13	5	33	Pr	27.3	75	7.99 × 10^4	1.36 × 10^7	7	6	No	0
14	5	33	Pr	27.3	75	8.53 × 10^4	1 × 10^7	1.5	6	No	0
From SEL Runs											
1	1	125	Pr	27.3	75	1.07 × 10^5	2 × 10^7	7	6	Yes	396
2	1	125	Pr	0	66.43	1.14 × 10^5	9.96 × 10^6	7	6	Yes	5
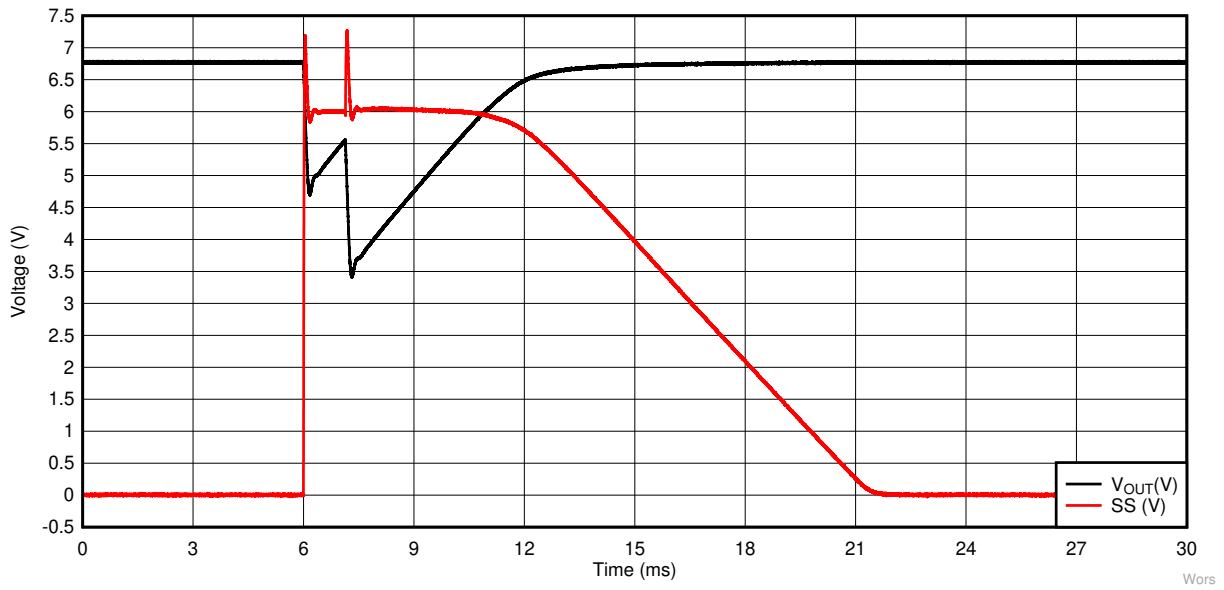
Figure 8-1. Worst Case Overlay of V_{OUT} and SS SET for Run 1 at LET_{EFF} 75 MeV × cm^2 / mg and T = 125°C

9 Total Ionizing Dose From SEE Experiments

The TPS7H2201-SP is rated for a total ionizing dose (TID) of 100 krad (Si). In the course of the SEE testing, the heavy-ion exposure delivered ≈10 krad (Si) per 10^7 ions/cm^2 run. The cumulative TID exposure for all units was controlled to be below the 100 krad(Si).

10 Orbital Environment Estimations

To calculate on-orbit SEE event rates, both the device SEE cross-section and the flux of particles encountered in a particular orbit are required. Device SEE cross-sections are usually determined experimentally while flux of particles in orbit is calculated using various codes. For the purpose of generating some event rates, a Low-Earth Orbit (LEO) and a Geostationary-Earth Orbit (GEO) were calculated using CREME96. CREME96 code, short for Cosmic Ray Effects on Micro-Electronics, is a suite of programs (10, 11) that enable estimation of the radiation environment in near-Earth orbits. CREME96 is one of several tools available in the aerospace industry to provide accurate space environment calculations. Over the years since its introduction, the CREME models have been compared with on-orbit data and demonstrated their accuracy. In particular, CREME96 incorporates realistic *worst-case* solar particle event models, where fluxes can increase by several orders-of-magnitude over short periods of time.

For the purposes of generating conservative event rates, the worst-week model (based on the biggest solar event lasting a week in the last 45 years) was selected, which has been equated to a 99%-confidence level worst-case event (12, 13). The integrated flux includes protons to heavy ions from solar and galactic sources. A minimal shielding configuration is assumed at 100 mils (2.54 mm) of aluminum. Two orbital environments were estimated, that of the International Space Station (ISS) which is LEO and the GEO environment. Figure 10-1 shows the integrated flux (from high LET to low) for these two environments.
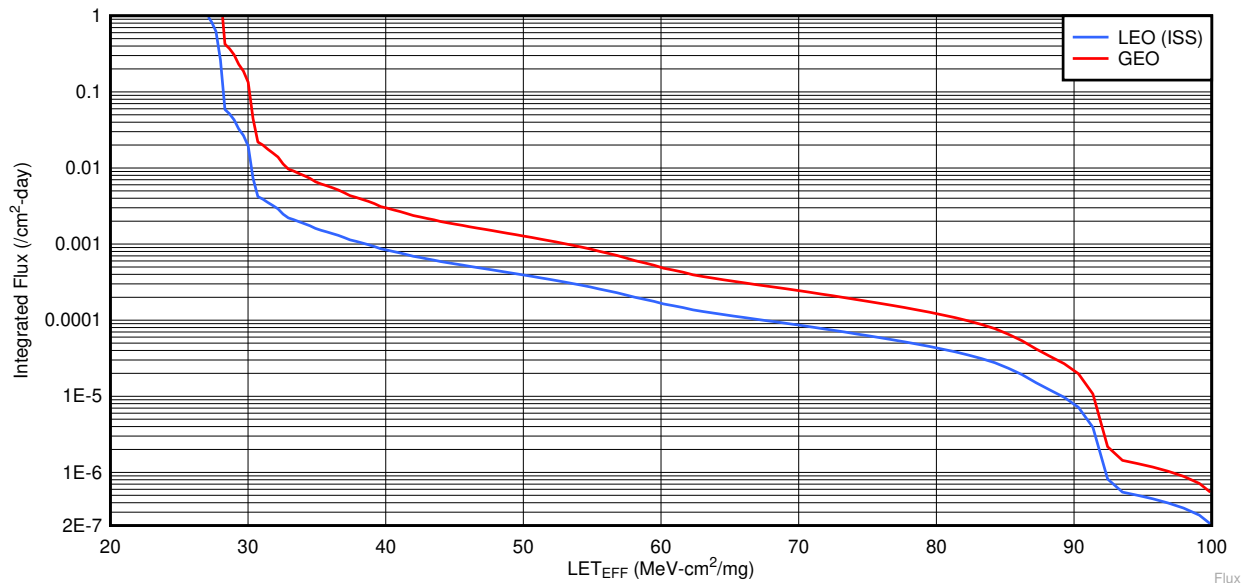

Figure 10-1. Integral Particle Flux Versus LETEFF for a LEO-ISS (blue curve) and a GEO (red curve) Environment as Calculated by CREME96 Assuming Worst-week and 100 mils (2.54 mm) of Aluminum Shielding

Note that the y-axis represents flux integrated from higher LET to lower LET. The value of integral flux at any specific LET value is actually the integral of all ion events at that specific LET value to all higher LETs.

Figure 10-1 shows the Integral Particle Flux versus LET_{EFF} for a LEO-ISS (blue curve) and a GEO (red curve) environment as calculated by CREME96 assuming worst-week and 100 mils (2.54 mm) of aluminum shielding. Note that the y-axis represents flux integrated from higher LET to lower LET. The value of integral flux at any specific LET value is actually the integral of all ion events at that specific LET value to all higher LETs.

Using this data, a user can extract integral particle fluxes for any arbitrary LET of interest. To simplify the calculation of event rates, assume that all cross-section curves are square, meaning that below the onset LET, the cross-section is identically zero while above the onset LET, the cross-section is uniformly equal to the saturation cross-section. Figure 10-2 shows the approximation, with the green curve as the actual Weibull fit to the data with the square approximation shown as the red-dashed line. This allows the user to calculate event rates with a single multiplication, the event rate becoming the product of the integral flux at the onset LET, and the saturation cross-section. Obviously this leads to an over-estimation of the event rate since the area under the square approximation is larger than the actual cross-section curve – but for the purposes of calculating upper-bound event rate estimates, this modification avoids the requirement of the integral over the flux and cross-section curves.
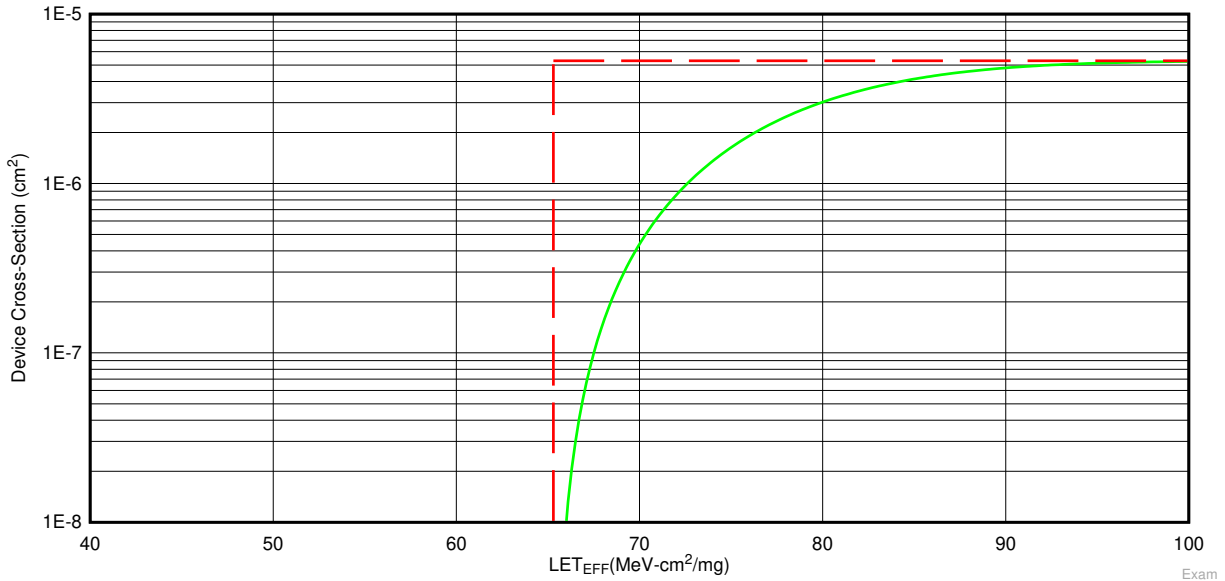
Figure 10-2. Device Cross-section Versus LET$_{EFF}$ Showing How the Weibull Fit (Green) is Simplified with the Use a Square Approximation (Red Dashed Line)

Figure 10-2 shows a device cross-section versus LET$_{EFF}$, showing how the Weibull fit (green) is simplified with the use of a square approximation (red dashed line).

To demonstrate how the event rates in this report were calculated, assume that the user must calculate an event rate for a GEO orbit for the device whose cross-section is shown in Figure 10-2. Using the red curve in Figure 10-1 and the onset LET value obtained from Figure 10-2 (approximately 65 MeV-cm^2 / mg), the GEO integral flux is approximately 3.24×10^{-4} ions / cm^2-day. The event rate is the product of the integral flux and the saturation cross-section in Figure 10-2 (approximately 5.3×10^{-6} cm^2):

$$GEO\ Event\ Rate = \left(3.24 \times 10^{-4}\ \frac{ions}{cm^2 \times day}\right) \times (5.3 \times 10^{-6}\ cm^2) = 1.71 \times 10^{-9}\ \frac{events}{day} \tag{6}$$

$$GEO\ Event\ Rate = 0.71 \times 10^{-10}\ \frac{events}{hr} = 0.071\ FIT \tag{7}$$

$$MTBF = 1{,}607{,}820\ Years \tag{8}$$

11 Confidence Interval Calculations

For conventional products where hundreds of failures are seen during a single exposure, you can determine the average failure rate of parts being tested in a heavy-ion beam as a function of fluence with a high degree of certainty and reasonably tight standard deviation, and thus have a good deal of confidence that the calculated cross-section is accurate.

With radiation hardened parts however, determining the cross-section becomes more difficult since often few, or even, no failures are observed during an entire exposure. Determining the cross-section using an average failure rate with standard deviation is no longer a viable option, and the common practice of assuming a single error occurred at the conclusion of a null-result can end up in a greatly underestimated cross-section.

In cases where observed failures are rare or non-existent, the use of confidence intervals and the Chi-Squared distribution is indicated. The Chi-Squared distribution is an optionh for the determining a reliability level when the failures occur at a constant rate. In the case of SEE testing, where the ion events are random in time and position within the irradiation area, you expect a failure rate that is independent of time (presuming that parametric shifts induced by the total ionizing dose do not affect the failure rate), and as a result, the use of Chi-Squared statistical techniques is valid (since events are rare an exponential or Poisson distribution is usually used).

In a typical SEE experiment, the device-under-test (DUT) is exposed to a known, fixed fluence (ions / cm^2) while the DUT is monitored for failures. This is analogous to fixed-time reliability testing and, more specifically, time-terminated testing, where the reliability test is terminated after a fixed amount of time whether or not a failure has occurred (in the case of SEE tests fluence is substituted for time and hence it is a fixed fluence test) [14]. Calculating a confidence interval specifically provides a range of values which is likely to contain the parameter of interest (the actual number of failures/fluence). Confidence intervals are constructed at a specific confidence level. For example, a 95% confidence level implies that if a given number of units were sampled numerous times and a confidence interval estimated for each test, the resulting set of confidence intervals would bracket the true population parameter in about 95% of the cases.

To estimate the cross-section from a null-result (no fails observed for a given fluence) with a confidence interval, you start with the standard reliability determination of lower-bound (minimum) mean-time-to-failure for fixed-time testing (an exponential distribution is assumed):

$$MTTF = \frac{2nT}{\chi^2_{2(d+1);100\left(1-\frac{\alpha}{2}\right)}}$$

(9)

where

- *MTTF* is the minimum (lower-bound) mean-time-to-failure
- *n* is the number of units tested (presuming each unit is tested under identical conditions)
- *T*, is the test time
- x^2 is the chi-square distribution evaluated at 100(1 − α / 2) confidence level
- d is the degrees-of-freedom (the number of failures observed)

With slight modification for this purpose, invert the inequality and substitute *F* (fluence) in the place of *T*:

$$MFTF = \frac{2nF}{\chi^2_{2(d+1);100\left(1-\frac{\alpha}{2}\right)}}$$

(10)

where

- *MFTF* is mean-fluence-to-failure
- *F* is the test fluence
- x^2 is the chi-square distribution evaluated at 100(1 − α / 2) confidence
- *d* is the degrees-of-freedom (the number of failures observed)

The inverse relation between MTTF and failure rate is mirrored with the MFTF. Thus the upper-bound cross section is obtained by inverting the MFTF:

$$\sigma = \frac{\chi^2_{2(d+1);100\left(1-\frac{\alpha}{2}\right)}}{2nF} \tag{11}$$

Assume that all tests are terminated at a total fluence of 10^6 ions / cm^2. Also assume that you have a number of devices with very different performances that are tested under identical conditions. Assume a 95% confidence level ($\sigma = 0.05$). Note that as *d* increases from 0 events to 100 events, the actual confidence interval becomes smaller, indicating that the range of values of the true value of the population parameter (in this case the cross section) is approaching the mean value + 1 standard deviation. This makes sense when one considers that as more events are observed the statistics are improved such that uncertainty in the actual device performance is reduced.

Table 11-1. Experimental Example Calculation of Mean-Fluence-to-Failure (MFTF) and, σ Using a 95% Confidence Interval

Degrees-of-Freedom (d)	2(d + 1)	χ^2 at 95%	CALCULATED CROSS SECTION (cm^2)		
			Upper-Bound at 95% Confidence	Mean	Average + Standard Deviation
0	2	7.38	3.69E–06	0.00E+00	0.00E+00
1	4	11.14	5.57E–06	1.00E–06	2.00E–06
2	6	14.45	7.22E–06	2.00E–06	3.41E–06
3	8	17.53	8.77E–06	3.00E–06	4.73E–06
4	10	20.48	1.02E–05	4.00E–06	6.00E–06
5	12	23.34	1.17E–05	5.00E–06	7.24E–06
10	22	36.78	1.84E–05	1.00E–05	1.32E–05
50	102	131.84	6.59E–05	5.00E–05	5.71E–05
100	202	243.25	1.22E–04	1.00E–04	1.10E–04

11.1 Rate Orbit Calculation

Event rates were calculated for LEO (ISS) and GEO environments by combining CREME96 orbital integral flux estimations and simplified SEE cross-sections according to methods shown in Section 10. A minimum shielding configuration of 100 mils (2.54 mm) of aluminum, and *worst-week* solar activity (this is similar to a 99% upper bound for the environment) was assumed. Using the 95% upper-bounds for the SEL, SEB/SEGR, and SET, the event-rates of the TPS7H2201-SP are listed in Table 11-2, Table 11-3, and *Table 11-4*, respectively. As previously mentioned, no SEL, SEB, or SEGR events were observed under any of the test runs, indicating that the TPS7H2001-SP is SEL, SEB, and SEGR immune. Cross-sections and event rates shown in Table 11-2 and Table 11-3, are calculated based on 0 events observed using a 95% (2σ) confidence interval.

Table 11-2. SEL Event Rate Calculations for Worst-week LEO and GEO Orbits

Orbit Type	Onset LET (MeV × cm² / mg)	CREME96 Integral Flux (/ day × cm²)	σ SAT (cm²)	Event Rate (/ day)	Event Rate (FIT)	MTBE (Years)
LEO (ISS)	75.0	6.61×10^{-5}	1.84×10^{-7}	1.22×10^{-11}	5.07×10^{-4}	2.25×10^{8}
GEO		1.87×10^{-4}		3.44×10^{-11}	1.43×10^{-3}	7.97×10^{7}

Table 11-3. SEB/SEGR Event Rate Calculations for Worst-week LEO and GEO Orbits

Orbit Type	Onset LET (MeV × cm² / mg)	CREME96 Integral Flux (/ day × cm²)	σ SAT (cm²)	Event Rate (/ day)	Event Rate (FIT)	MTBE (Years)
LEO (ISS)	75	6.61×10^{-5}	4.61×10^{-8}	3.05×10^{-12}	1.27×10^{-4}	8.99×10^{8}
GEO		1.87×10^{-4}		8.61×10^{-12}	3.59×10^{-4}	3.18×10^{8}

Table 11-4. SET Event Rate Calculations for Worst-week LEO and GEO Orbits

Orbit Type	Onset LET (MeV × cm² / mg)	CREME96 Integral Flux (/ day × cm²)	σ SAT (cm²)	Event Rate (/ day)	Event Rate (FIT)	MTBE (Years)
LEO (ISS)	75	6.61×10^{-5}	2.29×10^{-8}	1.51×10^{-12}	6.31×10^{-5}	1.81×10^{9}
GEO		1.87×10^{-4}		4.28×10^{-12}	1.78×10^{-5}	6.4×10^{8}

12 Summary

The purpose of this report is to summarize the TPS7H2201-SP heavy-ions SEE performance. The data shows that the TPS7H2201-SP is SEL free at VIN = 7 V, 6 A , T = 125°C, and LET_{EFF}= 75 MeV × cm^2 / mg. The data also shows that the device is SEB/SEGR free at VIN = 7 V, 6 A, T = 20–25°C and LET_{EFF} = 75 MeV-cm^2 / mg. The TPS7H2201-SP shows to be SET-free for all electrical conditions at room temperature. Worst case transient observed when the die temperature was 125°C is presented.

SLVAE32B – AUGUST 2018 – REVISED DECEMBER 2023
Submit Document Feedback

13 References

1. M. Shoga and D. Binder, "Theory of Single Event Latchup in Complementary Metal-Oxide Semiconductor Integrated Circuits", IEEE Trans. Nucl. Sci, Vol. 33(6), Dec. 1986, pp. 1714-1717.
2. G. Bruguier and J.M. Palau, "Single particle-induced latchup", IEEE Trans. Nucl. Sci, Vol. 43(2), Mar. 1996, pp. 522-532.
3. J. M. Hutson, R. D. Schrimpf, and L. W. Massengill, "The effects of scaling and well and substrate contact placement on single event latchup in bulk CMOS technology," in Proc. RADECS, Sept. 2005, pp. PC24-1– PC24-5.
4. N. A. Dodds, J. M. Hutson, J. A. Pellish, et al., "Selection of Well Contact Densities for Latchup-Immune Minimal-Area ICs, IEEE Trans. Nucl. Sci, Vol. 57(6), Dec. 2010, pp. 3575-3581.
5. D. B. Estreich and A. Ochoa, Jr., and R. W. Dutton, "An Analysis of Latch-Up Prevention in CMOS IC's Using an Epitaxial-Buried Layer Process*, Proceed. IEEE Elec. Dev. Meeting, 24, Dec. 1978, pp. 230-234.
6. G. H. Johnson, J. H. Hohl, R. D. Schrimpf and K. F. Galloway, "Simulating single-event burnout of n-channel power MOSFET's," in IEEE Transactions on Electron Devices, vol. 40, no. 5, pp. 1001-1008, May 1993.
7. J. R. Brews, M. Allenspach, R. D. Schrimpf, K. F. Galloway, J. L. Titus and C. F. Wheatley, "A conceptual model of a single-event gate-rupture in power MOSFETs," in IEEE Transactions on Nuclear Science, vol. 40, no. 6, pp. 1959-1966, Dec. 1993.
8. Texas A&M University, *Texas A&M University Cyclotron Institute Radiation Effects Facility*, webpage.
9. James F. Ziegler, *The Stopping and Range of Ions in Matter (SRIM) simulation tool*, webpage.
10. Vanderbilt University, *CREME-MC*, webpage.
11. A. J. Tylka, et al., "CREME96: A Revision of the Cosmic Ray Effects on Micro-Electronics Code", IEEE Trans. Nucl. Sci., 44(6), 1997, pp. 2150-2160.
12. A. J. Tylka, W. F. Dietrich, and P. R. Bobery, "Probability distributions of high-energy solar-heavy-ion fluxes from IMP-8: 1973-1996", IEEE Trans. on Nucl. Sci., 44(6), Dec. 1997, pp. 2140 – 2149.
13. A. J. Tylka, J. H. Adams, P. R. Boberg, et al.,"CREME96: A Revision of the Cosmic Ray Effects on Micro-Electronics Code", Trans. on Nucl. Sci, 44(6), Dec. 1997, pp. 2150 – 2160.
14. D. Kececioglu, "Reliability and Life Testing Handbook", Vol. 1, PTR Prentice Hall, New Jersey,1993, pp. 186-193.

14 Revision History

Submit Document Feedback

IMPORTANT NOTICE AND DISCLAIMER